4998–5011 *Nucleic Acids Research, 2012, Vol. 40, No. 11* *Published online 9 February 2012*
doi:10.1093/nar/gks070

The DEAD-box helicase DDX3 supports the assembly of functional 80S ribosomes

Rene Geissler, Ralph P. Golbik and Sven-Erik Behrens*

Institute of Biochemistry and Biotechnology, Faculty of Life Sciences (NFI), Martin Luther University Halle-Wittenberg, Kurt-Mothes-Str. 3, D-06120 Halle/Saale, Germany

Received November 9, 2011; Revised January 18, 2012; Accepted January 19, 2012

ABSTRACT

The DEAD-box helicase DDX3 has suggested functions in innate immunity, mRNA translocation and translation, and it participates in the propagation of assorted viruses. Exploring initially the role of DDX3 in the life cycle of hepatitis C virus, we observed the protein to be involved in translation directed by different viral internal ribosomal entry sites. Extension of these studies revealed a general supportive role of DDX3 in translation initiation. DDX3 was found to interact in an RNA-independent manner with defined components of the translational pre-initiation complex and to specifically associate with newly assembling 80S ribosomes. DDX3 knock down and *in vitro* reconstitution experiments revealed a significant function of the protein in the formation of 80S translation initiation complexes. Our study implies that DDX3 assists the 60S subunit joining process to assemble functional 80S ribosomes.

INTRODUCTION

Eukaryotic protein synthesis involves translation initiation, elongation, termination and the recycling of ribosomes. The canonical translation initiation process on capped mRNAs consists of two intricate steps that eventually lead to the assembly of 80S initiation complexes where the anticodon of an aminoacylated initiator tRNA (mostly Met–tRNAi) is base-paired with the mRNA's initiation codon in the ribosomal P(peptidyl)-site. In the current model [(1,2) and references herein; Figure 1], a pre-assembled 43S pre-initiation complex (PIC) that consists of a small 40S ribosomal subunit, the translation initiation factors eIF1, eIF1A, eIF3, conceivably eIF5 and the ternary eIF2-GTP-Met-tRNAi complex (TC), first associates with the 5′-region of the mRNA. During this process, structures in the mRNA's 5′-untranslated region (5′-UTR) are unwound in an ATP-dependent manner involving eIF4F and eIF4B. eIF4F is a protein complex that includes the cap-binding protein eIF4E, the helicase eIF4A and the 'scaffold' protein eIF4G, the latter of which binds to eIF3, eIF4E, eIF4A and the poly A binding protein PABP. Interactions of eIF4F with the cap (*via* eIF4E) and with PABP and the poly A tail (*via* eIF4G) generates a loop structure of the mRNA. The PIC then scans in 5′–3′ direction for translation initiation codons. A matching contact of an initiation codon with the anticodon in Met–tRNAi switches the scanning complex to a 'closed conformation' that is discernible as 48S complex. Subsequent dislocation of eIF1 leads to eIF5-mediated GTP-hydrolysis in the TC. In the second step of translation initiation, eIF5B triggers the attachment of the 60S subunit to the 48S complex and the simultaneous displacement of eIF2–GDP, eIF1, eIF3, eIF4A, eIF4B, eIF4G and eIF5. The initiation process is concluded by eIF5B-mediated GTP hydrolysis and release of eIF1A and GDP-bound eIF5B from the assembled, elongation-competent 80S ribosome. The next codon-complementary aminoacyl–tRNA may now associate into the A(aminoacyl)-site of the ribosome and the first peptide bond may be produced.

The genomes of positive-strand RNA viruses in particular contain highly structured internal ribosomal entry sites (IRES) that enable non-canonical interactions of initiation factors and/or of the 40S ribosomal subunit and cap-independent ribosomal recruitment to internal RNA locations. Thus, in the case of the IRES encoded by the 5′-region of the hepatitis C virus (HCV) RNA genome, the 43S PIC directly attaches to the RNA in the absence of scanning and without the participation of eIF1, eIF1A, eIF4B and eIF4F (3,4).

A protein that has been implicated to contribute to the translation initiation process is the multifunctional DEAD-box helicase DDX3. DDX3 was found to be part of cytoplasmic complexes containing eIF2, eIF3, eIF4A, eIF4E and PABP, and mRNA translation was affected by DDX3 overexpression or DDX3 knock down. However, some data suggested that DDX3 acts as a translational suppressor while others indicated DDX3

*To whom correspondence should be addressed. Tel: +49 3455524960; Fax: +49 3455527387; Email: sven.behrens@biochemtech.uni-halle.de

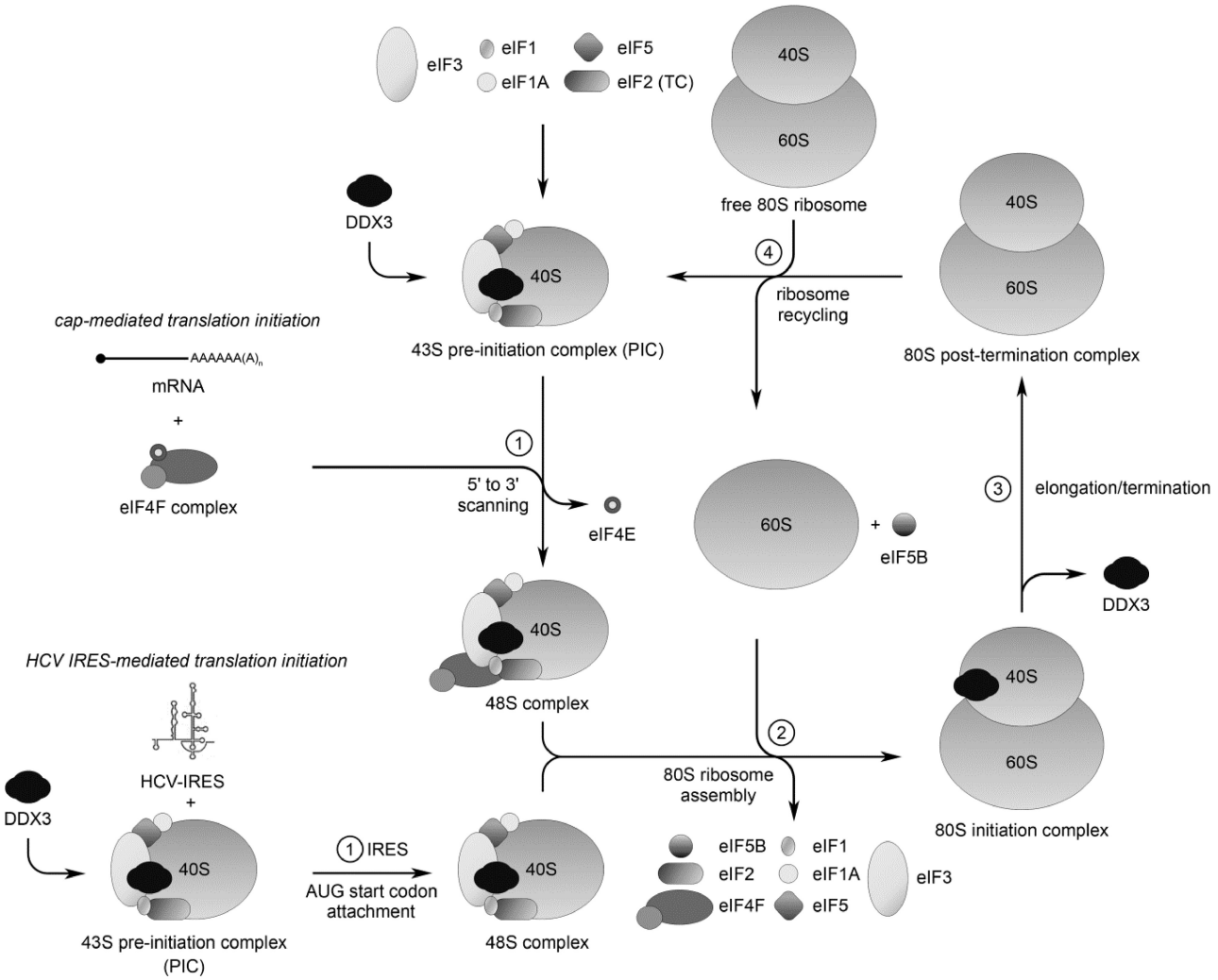

Figure 1. Models of cap- and HCV IRES-directed translation; suggested participation of DDX3 in translation initiation. Canonical (cap-mediated) translation is depicted in four stages; ① and ② represent the translation initiation process (see text). ① Binding of the 43S PIC and initiation factors to the 5′-end of mRNA and formation of the 48S complex (5′–3′ interactions of the mRNA not shown). ② Joining of 60S and assembly of the 80S translation initiation complex. ③ Elongation and termination phase resulting in 80S post-termination complexes. ④ Recycling of 80S post-termination complexes and of free 80S ribosomes. In HCV IRES-directed translation initiation, the 43S PIC directly binds to the AUG initiation codon in the absence of eIF4F and without scanning to assemble the 48S complex ①. Our data suggest that DDX3 joins the 43S PIC *via* direct (non-RNA mediated) interactions with eIF3 and the 40S subunit. This complex assembles with the mRNA to generate the 48S complex. DDX3 then is involved in conformational changes that favor the release of translation initiation factors and the joining of the 60S subunit. DDX3 remains bound to the 80S translation initiation complex but disassembles prior to the elongation process.

as a supportive translation factor that gives preference to mRNAs with structured 5′-UTR (5–8). This study was set out to further elucidate the role of DDX3 in translation. Applying different experimental systems, we obtained complementary evidence indicating that DDX3 represents a general, auxiliary translation factor that is involved in the second step of the translation initiation process.

MATERIALS AND METHODS

Plasmids

The HCV constructs were derived from pSGR-JFH1 encoding the bi-cistronic replicon (kindly provided by Dr Wakita, Tokyo Metropolitan Institute for Neuroscience). Details on construction and transcription of the plasmids used in this study are supplied as Supplementary Data.

Cell culturing, transfection conditions, luciferase assay

Human hepatoma (Huh7) and human embryonic kidney (HEK293T-REx) cells were grown in DMEM (Invitrogen) supplemented with 10% FCS, 1% non-essential amino acids and 1% pen/strep (Invitrogen). Selection and culturing of Huh7 cell lines that contained the HCV bi-cistronic replicon was performed with 800 μg G418 (Invitrogen)/ml culture medium. For siRNA transfection, 70% confluent Huh7 cells were transfected with 1200 pmol siRNA using Lipofectamine RNAiMax (Invitrogen) and a

1:40 Lipofectamine (μl)/RNA (pmol) ratio (siRNAs listed in Supplementary Table S2). For plasmid transfection 50% confluent HEK cells were transfected with 20 μg plasmid DNA/10 ml growth medium using Turbofect (Fermentas). Double RNA transfections were performed such that the cells were first transfected with siRNA and, 72 h later, re-transfected with 4 pmol of luciferase reporter RNA or 200 ng (80 fmol) of HCV-JFH1 mono-cistronic replicon RNA using the electroporation protocol of Grassmann *et al.* (9). Huh7 transfected with the HCV-JFH1 mono-cistronic replicon were harvested 48 h post-transfection to analyze HCV RNA and proteins levels. Huh7 cells transfected with reporter RNAs were harvested at 1 h post-transfection and luciferase assays (Promega) performed.

Quantitative RT–PCR

qRT–PCR was performed as described by Geissler *et al.* (10) (see primers in Supplementary Table S1). For normalization of the relative levels of immunoprecipitated mRNAs ($E^{\Delta\Delta Ct}$) shown in Figure 4, the precipitates were supplemented with 5 fmol of 5′-cap-Luc-poly A RNA and the determined levels of RNA adjusted to this internal control.

Preparation of S10 extracts and *in vitro* translation assays

Translation-competent cytoplasmic (S10) extracts of Huh7 cells were prepared essentially as described by Yu *et al.* (11). For reporter assays, 60 fmol of the luciferase-encoding RNAs were incubated 30 min in the extract. S10 extracts of siRNA-treated Huh7 cells were prepared 72 h post-transfection of the cells with siRNA. In the indicated cases, endogenous RNAs were removed by treating the extracts with 0.08 Units/μl micrococcal nuclease (Roche) for 15 min at 25°C. Cell lysates for western blots were prepared following the protocol of Isken *et al.* (12).

Immunoprecipitation

An amount of 4 μl of DDX3 antiserum or preimmune serum were bound to 30 μl (1:1 suspension) of protein A-sepharose (Amersham). In IBB1 buffer (20 mM HEPES pH 7.6, 150 mM KCl, 0.5% NP40, 1 mM DTT), the beads were incubated for 4 h at 4°C with 150 μg of total protein of extracts of naïve or replicon-transfected Huh7 cells. For a total digestion of RNA, 100 μg/ml RNase A (Roche) was added. The beads were washed three times with IBB1 and the proteins denatured in 20 μl SDS sample buffer. For the analysis of RNA, the precipitate was digested with proteinase K and the RNAs extracted and precipitated. Flag-immunoprecipitation of DDX3 was performed from lysates of HEK293 cells using ANTI-FLAG M2 Affinity Gel (Sigma) and the manufacturer's instructions. In the second round of the assay, the precipitated Flag-DDX3 was further incubated with purified 43S components in IBB2 buffer (50 mM Tris pH 7.5, 150 mM NaCl) for 3 h at 4°C.

Purification of 40S/60S, eIFs and DDX3

40S and 60S ribosomal subunits, eIF2, recombinant eIF1, eIF1A, eIF5, $eIF5B_{587–1220}$ and *Escherichia coli* methionyl tRNA synthetase were purified essentially as described by Pisarev *et al.* (13). During purification of eIF1A, eIF5 and *E. coli* methionyl tRNA synthetase, MonoQ HR 5/5 was replaced by ResourceQ (Amersham Biosciences). During purification of eIF1 and $eIF5B_{587–1220}$, MonoS HR 5/5 and MonoQ HR 5/5 were replaced by HiTrap Heparin HP (GE Healthcare). All proteins were finally applied to HiLoad 16/60 Superdex 75 (GE Healthcare) equilibrated with 20 mM Tris pH 7.5, 100 mM KCl, 1 mM DTT, 0.1 mM EDTA and 10% glycerol. eIF2 and eIF3 were purified from HeLa extract as described by Damoc *et al.* (14) and Pisarev *et al.* (13), respectively. Flag-DDX3 was purified 36 h after transfection of HEK293T-REx cells with pcDNA5/TO Flag-DDX3 using ANTI-FLAG M2 Affinity Gel (Sigma). Recombinant DDX3 (ε = 74260/M cm) was purified from *E. coli* inclusion bodies according to Stoyan *et al.* (15). The recombinant protein was not applicable in functional assays; it was used for quantification purposes (Figure 6).

Translation initiation assay

[^{32}P]-labeled RNA was incubated in S10 extract under translation conditions at 37°C in the presence of 2 mM cycloheximide (AppliChem). The reactions were stopped on ice and loaded on a 5–25% (w/v) linear sucrose gradient containing 20 mM HEPES pH 7.6, 150 mM K-Acetat, 5 mM $MgCl_2$ and 1 mM DTT. Gradients were centrifuged in a Beckman SW40Ti rotor at 38 000 rpm for 2 h at 4°C and harvested at 600 μl fractions (bottom-top). The OD_{260} was determined and radioactivity measured by Čerenkov counting. For protein analyses, 400 μl of each fraction were precipitated with TCA and the protein content analyzed by SDS–PAGE and western blot. For separation of the ribosomal subunits, the S10 extract was supplemented with 25 mM EDTA prior to centrifugation in gradient buffer containing 25 mM EDTA. Centrifugation was carried out in a Beckman SW40Ti rotor at 38 000 rpm for 4 h at 4°C. For polysomal analyses, the Huh7 cells were incubated with 2 mM cycloheximide for 15 min prior to preparation of S10 extract (again in the presence of 2 mM cycloheximide). The extract was loaded on a 15–45% linear sucrose gradient supplemented with 0.4 mM cycloheximide and centrifuged at 30 000 rpm for 2 h at 4°C (16).

Aminoacylation of $tRNA_i^{Met}$, *in vitro* assembly and analysis of translation initiation complexes

Aminoacylation of $tRNA_i^{Met}$ and *in vitro* assembly of 48S and 80S complexes were performed as described by Pisarev *et al.* (13). The 48S complexes on HCV 5′-UTR–sORF–3′-UTR RNA were assembled by incubating 5 pmol RNA with 5 pmol of *in vitro* transcribed and aminoacylated Met–$tRNA_i^{Met}$, 4 pmol eIF3, 3 pmol Flag-DDX3 and 3 pmol 40S subunit in a 40 μl reaction in buffer 20 mM Tris pH 8.0, 100 mM K-Acetat, 2.5 mM $MgCl_2$ and 1 mM DTT supplemented with 1 mM ATP

and 0.2 mM GTP for 10 min at 37°C. For 80S assembly, 48S complexes were further incubated with 5 pmol $eIF5B_{587–1220}$ and 3 pmol 60S subunit for 2 min at 37°C. Concentrations of the ribosomal subunits and proteins were determined by OD_{260} and OD_{280} measurements. Initiation complexes were analyzed by 5–25% (w/v) linear sucrose gradient centrifugation in a Beckman SW40Ti rotor at 38 000 rpm for 2 h at 4°C.

Western blotting

The applied antibodies were purchased from Santa-Cruz Biotechnology (eIF2α, sc-11386; eIF3c, sc-28858), Abcam (Neomycin phosphotransferase II, ab 60018), BD (eIF6, 611120), Cell Signaling Technology (rpS3, 2579; rpS6, 2317), Bethyl Laboratories (rpL26, A300-686A), Novagen (His-Tag-Antibody, 71841) and Sigma (vinculin, V9131). The rabbit antiserum against DDX3 was described by Angus *et al*. (17). The applied NS5A antibody was produced against recombinant NS5A (Eurogentec). The antibody recognizing IGF2BP1/2 was from Dr Hüttelmaier (University of Halle). Secondary antibodies (HRP) were purchased from GE Healthcare. Western blots were performed following the manufacturer's instructions. For quantification, the signals were evaluated by the program Image Quant.

Data evaluation and statistics

The data evaluation of the experiments including the number of experiments are indicated in the respective figure legends. Based on the nature of the subject and the inter-experimental variability, a common data normalization procedure was performed that related both the value of the control and of the treatment group to the value of the control for each independent experiment. A statistical data analysis was not performed if the normalized control values (0% or 100%, 0 or 1) did not display any variance. Statistics (two-sided unpaired *t*-test) was performed where normalization considered the relation of the absolute values to the mean of the control.

RESULTS

DDX3 is a functional determinant of IRES-mediated translation

Earlier RNA–protein interaction studies and siRNA knock down screens of others and us showed that DDX3 interacts in a yet unknown manner with the UTRs of the HCV RNA genome, and that the protein is indispensable for viral replication (18–21). This study was originally aimed at further investigating the function of DDX3 in the HCV life cycle, and it was initiated by testing the effect of a siRNA-directed intracellular depletion of DDX3 ('DDX3 knock down') on HCV replication. For this purpose, we first used Huh7 cells that were persistently transfected with a subgenomic, 'bi-cistronic' HCV replicon RNA [HCV subtype 2A 'JFH'; (22); Figure 2A]. In the bi-cistronic HCV replicon, the HCV IRES directs the translation of a neomycine/geneticin (Neo) resistance gene while synthesis of the viral replicase proteins is enabled by the IRES of encephalomyocarditis virus (EMCV). The DDX3 knock down was achieved by transfection of the Huh7/HCV replicon cells with two different siRNAs, each causing a reduction of cytoplasmic DDX3 to ~15–25% of the original protein level at 72 h post-transfection (Figure 2C). Importantly, this moderate depletion of DDX3 had no impact on the cellular growth rate. DDX3 knock down with each of the two siRNAs did not affect the replication of the bi-cistronic HCV replicon in comparison to control cells (Figure 2B). However, immunoblotting revealed that the expression levels of Neomycin phosphotransferase as well as that of the HCV-encoded proteins (Figure 2C; reduction of HCV proteins exemplified by NS5A) were considerably lowered in both types of DDX3 knock down cells.

It was previously reported that in DDX3-depleted cells the replication of transiently transfected full-length HCV genomic RNA was strongly reduced while this effect was less pronounced in persistently replicon-transfected cells (19,20). Accordingly, we next investigated the effect of DDX3 knock down on the replication of transiently transfected 'mono-cistronic' HCV replicon. Mono-cistronic HCV replicons resemble the genomic viral RNA such that translation of the NS proteins and RNA replication are exclusively governed by the authentic HCV UTRs (9) (Figure 2A). Huh7 cells were first transfected with the anti-DDX3 siRNAs, and 72 h later, re-transfected with the *in vitro* transcribed HCV RNA. After 48 h, the cells were harvested and the HCV RNA and protein content analyzed. Control experiments ensured that comparable amounts of RNA were transfected in each experiment (see Supplementary Figure S1). Thus, in contrast to the data obtained with the established cell line persistently expressing HCV replicon we found a strong reduction of HCV replication in the DDX3 knock down cells that had been transiently transfected with the replicon RNA (Figure 2D). As before, a significantly lowered level of viral protein expression was observed (Figure 2E).

These data suggest that DDX3 is an important functional determinant of HCV IRES- as well as EMCV IRES-mediated translation. The apparently contradictory effect of the DDX3 depletion on viral replication in transiently as opposed to stably transfected cell line is likely due to the fact that the former lack *de novo* synthesis of the viral replicase proteins which are necessary for the replication of the viral genome. This is not the case with the persistently transfected cells where a pre-existing abundance of the viral proteins would conceivably sustain viral RNA replication even in the face of DDX3 depletion (23).

DDX3 is generally involved in translation

To next assess DDX3 for a general role in translation, we generated different types of luciferase-encoding reporter RNAs: i.e. a capped model mRNA (+/− poly A tail), a capped RNA that contained the 5′- and 3′-UTRs of the West Nile virus (WNV) RNA genome, and RNAs that contained the 5′-UTRs of the EMCV (+/− poly A tail) and HCV genomes (+/− HCV 3′-UTR), respectively (Figure 2F and G; EMCV and WNV data in

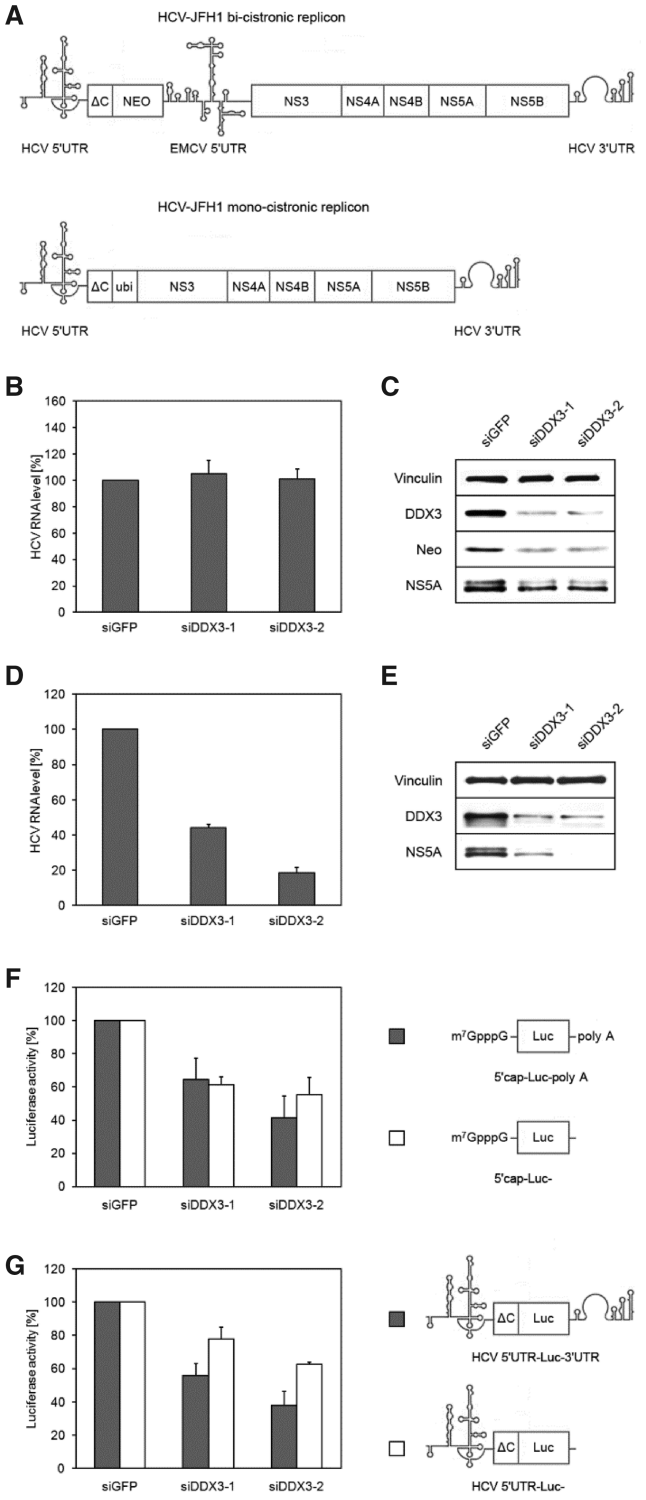

Figure 2. DDX3 is involved in translation. (**A**) Schematic representation of HCV replicons used in this study. The subgenomic viral RNAs encode all RNA elements and viral non-structural (NS) proteins (processed by the viral protease NS3/4A) enabling autonomous replication in the cytoplasm of transfected host cells. The UTRs are drawn as lines displaying the proposed RNA secondary structures; genetic units are boxed. (Upper panel) Bi-cistronic RNA replicon. Expression of the NEO selection marker enables the generation of G418-resistant replicon-containing cell lines (45). (Lower panel) Mono-cistronic RNA replicon. ΔC: HCV core-coding sequence element that supports efficient HCV IRES-mediated translation. ubi: ubiquitin-coding sequence enabling processing of the NS3 N-terminus by ubiquitincarboxyhydrolase. (**B**) Replication of the bi-cistronic HCV replicon in stably transfected Huh7 cells at 72 h post-transfection of two different anti-DDX3 siRNAs (siDDX3-1, siDDX3-2) and a control siRNA (siGFP), respectively. The viral RNA levels were measured by qRT–PCR. (**C**) Representative western blots showing the levels of DDX3, Neomycine phosphotransferase II and HCV NS5A in the cell cytoplasm after treatment with the indicated siRNAs. The vinculin levels served as controls. (**D**) Replication of the mono-cistronic HCV replicon in transiently transfected Huh7 cells at 72 h post-transfection of the indicated siRNAs. (**E**) Representative western blots of indicated proteins in cytoplasmic extracts of Huh7 cells that had been transfected with the indicated siRNAs and HCV mono-cistronic RNA replicon. (**F**, **G**) (Right) Schematic representation of the (F) mRNA and (G) HCV luciferase reporter constructs. The UTRs are drawn as lines with proposed RNA structures; the genetic unit encoding firefly luciferase is boxed. (Left) Luciferase activity assays. The reporter RNA transcripts were transfected into Huh7 cells 72 h after previous transfection with the indicated siRNAs. One hour post-transfection, the luciferase activity was determined in the cell lysates. The activity measured after transfection of the respective transcripts into control cells (that had been previously transfected with siGFP RNA) was set 100%. Error bars indicate standard deviation of four independent experiments.

Supplementary Figure S2). The RNAs were transfected into naïve and DDX3-depleted Huh7 cells and luciferase activity was measured in the cell lysates. Each reporter RNA was confirmed to exhibit equivalent amounts under the siGFP, siDDX3-1 and siDDX3-2 conditions (Supplementary Figure S3). Interestingly, in the DDX3-depleted cells, protein synthesis was reduced with all reporter RNAs tested to ~30–60% of the levels in control cells (Figure 2F, G and Supplementary Figure S2).

The comparable negative effect of the DDX3 knock down on the translation of each of the different reporter mRNAs (i.e. cap and IRES-containing mRNAs) implicated a general role of the protein in translation. Associated with these observations, a function of the protein in the cap-specific scanning process could be excluded, since neither HCV IRES- nor EMCV IRES-mediated translation require scanning to assemble 48S complexes (24–26). The impact of DDX3 on translation was further established to be independent of the presence of a poly A tail in the mRNA or, in the case of the HCV RNA, an authentic viral 3′-UTR.

A general role of DDX3 in translation was further supported by experiments where we transiently overexpressed the wild-type (wt) protein as well as a variant with disrupted ATPase and helicase functions in Hek293 cells. Subsequent transfection of these cells with the capped- or HCV UTR-containing reporter RNAs revealed a positive stimulation of translation by the wt protein. Interestingly, also the mutant DDX3 had a comparable activity indicating that the known enzymatic functions of the protein are not required for its supportive function in translation (see Supplementary Figure S4 and Discussion section).

DDX3 interacts with the 40 S ribosomal subunit

To examine DDX3 for functional contacts with the translation machinery we applied translation-competent cytoplasmic (S10) extracts from Huh7 cells that were prepared according to the protocol of Yu *et al.* (11).

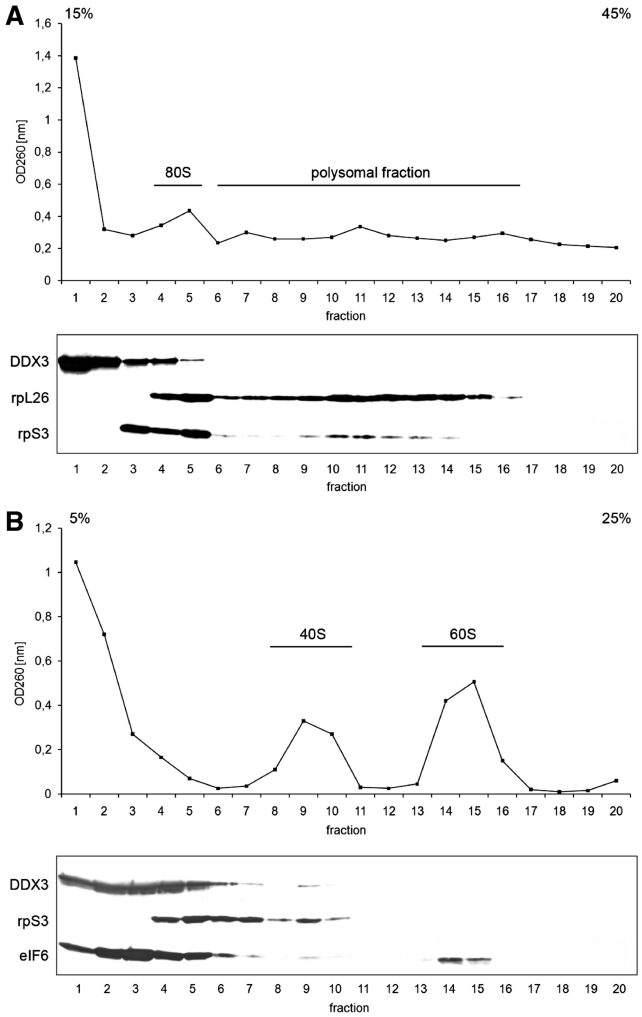

Figure 3. DDX3 interacts with the 40S ribosomal subunit. (**A**) Huh7 S10 cell extract was prepared in the presence of cycloheximide and subjected to 15–45% sucrose gradient centrifugation in the presence of cycloheximide. (Upper panel) OD_{260} values measured for each fraction. The monosomal 80S and polysomal fractions are indicated. (Lower panel) Fractionation of DDX3, rpS3 and rpL26 in the gradient was monitored by western blot. (**B**) Huh7 S10 extract was supplemented with EDTA and fractionated by 5–25% sucrose gradient centrifugation. (Upper panel) OD_{260} values measuring the RNA content are plotted versus the fraction numbers; sedimentation of the ribosomal subunits (40S, 60S) is indicated. (Lower panel) Fractionation of DDX3, rpS3 and eIF6 were monitored by western blot.

Testing first for interactions of DDX3 with 80S ribosomes or elongating polysomes, the extracts were prepared in the presence of the elongation inhibitor cycloheximide and fractionated by polysome sucrose gradient centrifugation (16). 80S ribosomes and polysomes were identified *via* the rRNA content in the gradient fractions and by immunoblot-probing for the ribosomal proteins rpS3 (40S component) and rpL26 (60S component); both ribosomal proteins were detectable in the 80S as well as in the polysomal fractions (Figure 3A). Probing for DDX3 revealed that most of the protein remained in the upper (less concentrated) gradient fractions and that a small quantity of the protein tailed into the 80S fractions. DDX3 was untraceable in the polysome fractions (Figure 3A).

To examine if DDX3 was interacting with one of the ribosomal subunits, we dissociated the 80S ribosomes in the Huh7 S10 extract by EDTA-treatment and separated the subunits by gradient centrifugation. The sedimentation profiles were measured again *via* the rRNA content and by immunoblot-testing for DDX3, rpS3, and eIF6. eIF6, a proposed ribosomal anti-association factor, is known to remain primarily attached to the 60S subunit (27). As shown in Figure 3B, high amounts of unbound DDX3 and eIF6 floated in the upper gradient fractions, and also rpS3 was found in these fractions. The latter observation could be attributable to the partial EDTA-mediated disruption of ribosomes, since in all other centrifugation analyses of this study, rpS3 sedimented exclusively with the 40S subunit and with the high molecular weight translation initiation complexes, respectively (e.g. Figure 5B). However, rpS3 and eIF6 were also present in the 40S fraction, and a portion of eIF6 sedimented, as expected, in the 60S fractions. DDX3 was not found at 60S but a small amount of the protein cofractionated with the 40S subunits (Figure 3B).

These results excluded DDX3 as a component of polysomes but revealed that a fraction of the protein associated with the 40S ribosomal subunit and, perhaps, with 80S ribosomes. We therefore reasoned that DDX3 was not participating in the elongation or termination phase of the translation process (Figure 1 step ③). Rather, the protein is likely to be a functional component of the translation initiation reaction active up to the assembly of functional 80S ribosomes or that it participates in ribosome recycling (Figure 1 steps ①, ② or ④).

DDX3 specifically interacts with components of translation initiation complexes

Earlier studies already suggested interactions of DDX3 with the translation initiation machinery (5–7). To specify these findings, several experimental setups were applied. First, we performed immunoprecipitations (IP) of DDX3 from the cytoplasmic Huh7 S10 extracts and analyzed the precipitate for associated translation initiation factors by western blot. Thus, in comparison to control IPs with preimmune serum, DDX3 specifically coprecipitated with eIF3 confirming the data of Lee *et al.* (6). Moreover, the 40S component rpS6 coprecipitated with DDX3 (Figure 4A). Notably, these interactions of DDX3 with eIF3, and, presumably, 40S, were detected irrespective of whether the experiment was performed in the absence or presence of RNase. This was in contrast with the RNA-binding proteins IGF2BP1/2, which coprecipitated with DDX3 only in the absence of RNase (Figure 4A).

These data revealed stable, RNA-independent interactions of DDX3 with different components of the 43S PIC. During translation initiation, 43S further evolve to mRNA-containing 48S complexes (Figure 1); DDX3 was hence assumed to be also part of the 48S complexes. As this would imply an association of the protein with various types of mRNAs, we repeated the IP with the

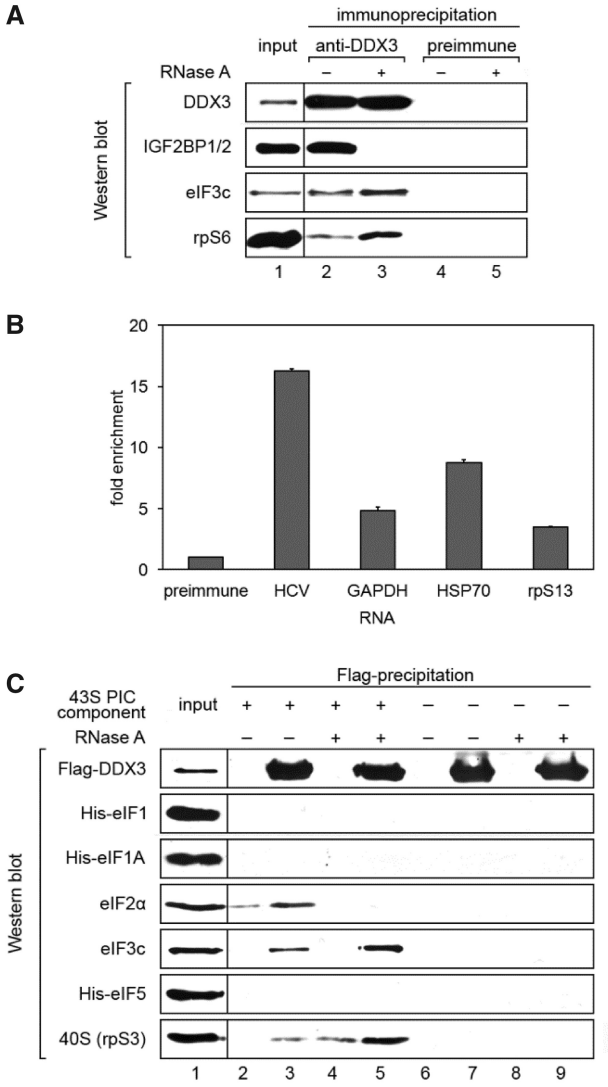

Figure 4. DDX3 interacts with the translation machinery. (**A**) DDX3 was immunoprecipitated from a defined amount of Huh7 S10 extract (input; lane 1) in the absence (−) or presence (+) of RNase A (lanes 2 and 3). Mock precipitations with preimmune serum (lanes 4 and 5) served as control. The indicated proteins in the input and precipitated samples were identified by immunoblotting using specific antibodies. (**B**) DDX3 was immunoprecipitated from extracts of Huh7 cells that were previously transfected with HCV mono-cistronic replicon RNA. The precipitate was analyzed for the indicated RNAs using specific qRT–PCR. The relative levels of coprecipitated RNAs were normalized to a defined amount of RNA that was prior added to the extract. The bar diagram represents the differences in the measured levels of the indicated RNAs (i.e. factors of enrichment) in comparison to control IPs with preimmune serum. Errors bars represent standard deviations of three independent experiments. (**C**) Flag-DDX3 was purified with anti-Flag antibody and applied to precipitation assays with anti-Flag antibody in the absence (lanes 7, 9) and presence (lanes 3, 5) of the individual, purified components of the 43S PIC (see Supplementary Figure S9). The PIC components and Flag-DDX3 were monitored by western blot with antisera directed against individual proteins (see input control, lane 1). As negative controls, the precipitations were carried out with fractions of Hek293 cells that expressed the untagged DDX3 ('mock control'; lanes 2, 4, 6, 8; see also Supplementary Figure S9). The precipitation assays were performed in the absence (lanes 2, 3, 6, 7) and presence (lanes 4, 5, 8, 9) of RNase A. Note that in the presence of RNase, components of the 40S subunit (indicated by rpS3) associated non-specifically with the applied sepharose beads (lane 4). One representative western blot for precipitated Flag-DDX3 is shown; only 10% of total input is shown.

DDX3-specific antiserum and S10 extracts of Huh7 cells that had been transiently transfected with HCV replicon and tested for coprecipitated RNAs by RT–PCR. In comparison to the controls, the HCV RNA was found to be ~16-fold enriched in the DDX3 precipitates. Likewise, the mRNAs of GAPDH and HSP70 (each containing highly structured 5′UTRs) as well as the mRNA of rpS13 (containing an unstructured 5′UTR) were coprecipitated and found enriched over the control by 5-, 9- and 3.5-fold, respectively (Figure 4B).

In the final experiment of this series, we tested DDX3 for direct interactions with individual components of the 43S PIC. Since DDX3 prepared from *E. coli* was non-applicable in these assays, a Flag-tagged version of the protein was overexpressed in Hek293 cells and purified with anti-Flag antibody. The purification was performed at stringent conditions to remove all associating proteins, and the Flag-DDX3 ensured to be free of components of the translation machinery (see Supplementary Figure S9D and S9E, and below). In a second, affiliated precipitation assay, which was performed again in the absence and presence of RNase, each component of the 43S PIC (eIF1, eIF1A, eIF2, eIF3, eIF5 and 40S ribosomal subunits) was individually tested for binding to the precipitated Flag-DDX3 (Supplementary Figure S9 shows the quality of the purified components). Coprecipitated components of the 43S PIC were identified by western blot; as a negative control we applied a mock purification where DDX3 was expressed without tag to the precipitation assays. As shown in Figure 4C, also in this constellation we observed a stable, RNA-independent association of DDX3 with eIF3. Conversely, eIF2 coprecipitated with DDX3 only in the absence of RNase. In addition, we obtained further evidence for protein-mediated interactions of DDX3 with components of the 40S ribosomal subunit, though purified 40S had the tendency to bind non-specifically to the applied sepharose beads. DDX3 did not directly interact with eIF1, eIF1A or eIF5 (Figure 4C).

The obtained results supported the idea of specific, functional interactions of DDX3 with the 43S PIC. These interactions were shown to occur in an RNA-independent manner and to specifically involve eIF3 and the 40S ribosomal subunit. The finding that different types of mRNAs coprecipitated with DDX3 was taken as an indication that the protein is also part of 48S translation initiation complexes.

DDX3 joins newly assembled 80S ribosomes

To test DDX3 for a specific function in translation initiation, we treated the translation-competent Huh7 S10 extract with cycloheximide to block elongation. Then, translation was initiated on a capped and on an HCV IRES-containing [^{32}P]-labeled mRNA substrate, respectively (see Figure 5A; the HCV data are provided as Supplementary Figure S5). The reactions were stopped at two time points and formation of the 48S and 80S translation initiation complexes analyzed by gradient centrifugation and by detection of rpS3 and of the labeled mRNA (Figure 5B).

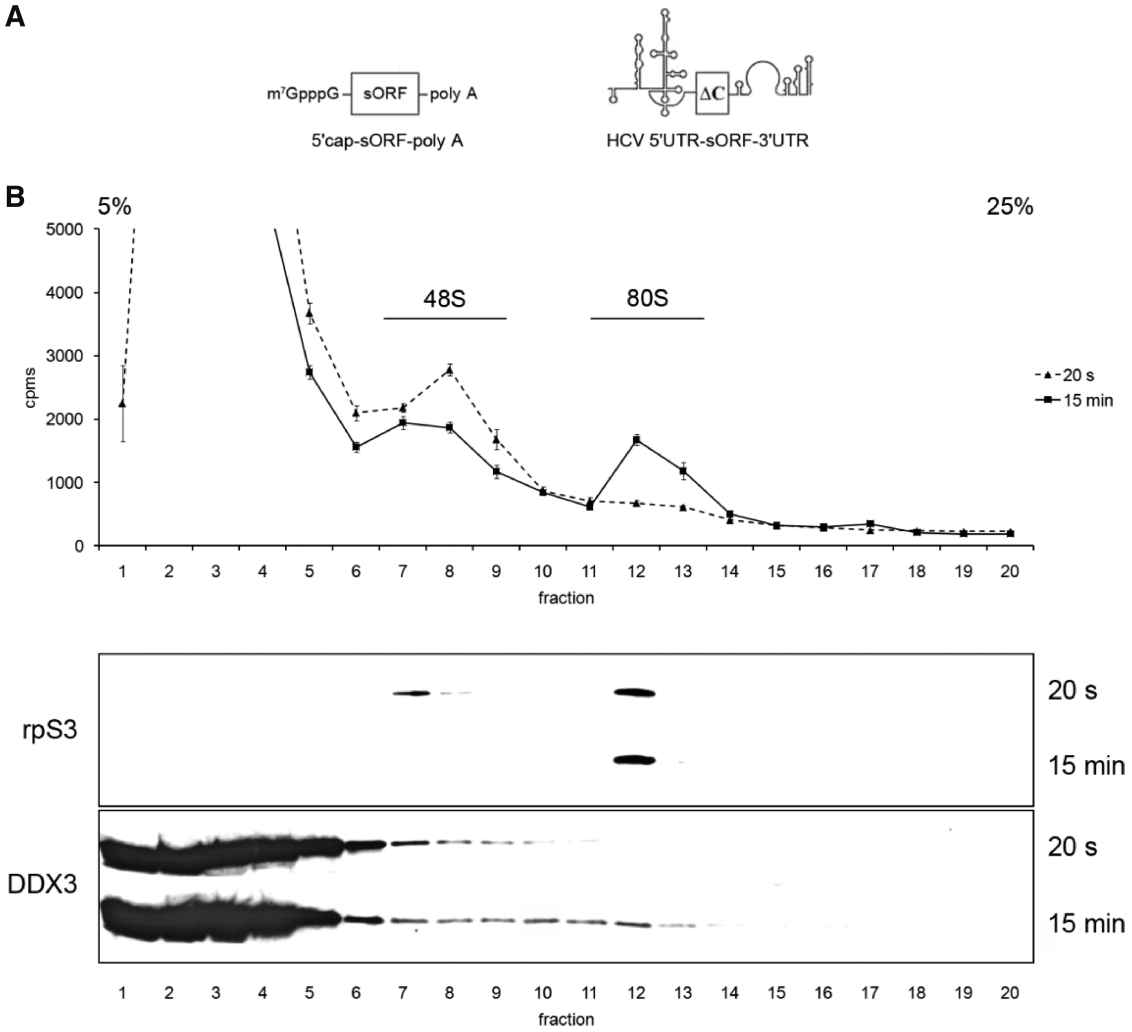

Figure 5. DDX3 specifically interacts with newly assembled 80S ribosomes. (**A**) Organization of the capped and HCV IRES-containing mRNA substrates used in these and the following studies. (**B**) Translation initiation assays were carried out with Huh7 S10 extracts for the indicated time frames in the presence of cycloheximide. The translation initiation complexes were fractionated by 5–25% sucrose gradient centrifugation and located *via* the supplemented [^{32}P]-labeled 5′-cap-sORF-poly A RNA transcript. (Upper panel) Sedimentation of the exogenous mRNA at 20 s (dashed line, triangles) and 15 min (continuous line, squares), respectively; the measured radioactivity was plotted versus the gradient fractions. The positions of 48S and 80S complexes are indicated. (Lower panel) Fractionation of DDX3 and rpS3 in the gradient monitored by western blot (for comparison, see Supplementary Figure S5). Errors bars represent standard deviations of three independent experiments.

First, we performed the translation initiation reaction with an analytical quantity (20 nM) of labeled 5′cap-sORF-poly A mRNA and a defined amount of cycloheximide-containing extract that was otherwise untreated. Following a short incubation time of 20 s, the exogenous mRNA substrate was detectable in the fractions that contained mRNPs (gradient fractions 2–4) and 48S complexes (fractions 7 and 8) but not in the fractions that contained 80S ribosomes (e.g. fraction 12). Testing for the presence of DDX3 in the gradient at this early time point of translation initiation, a certain amount of the protein cosedimented with 48S but not with 80S complexes (Figure 5B). This picture changed considerably when the reaction time was extended to 15 min. Here, the exogenous mRNA and, interestingly, also a fraction of DDX3 cosedimented with the 80S complex (fractions 12 and 13) (Figure 5B; see also Figure 6A).

In the second experiment, we repeated the initiation assay with the same amount of cycloheximide-treated Huh7 extract but with a higher quantity (60 nM) of labeled HCV 5′-UTR-sORF-3′-UTR RNA (Supplementary Figure S5). Moreover, to monitor the assembly of initiation complexes solely on the exogenous HCV mRNA, all endogenous RNAs were removed by prior treatment of the extract with micrococcal nuclease (MN). Thus, we obtained essentially the same results as with the capped mRNA transcript, namely a translocation of DDX3 into 80S ribosomes, but only if these ribosomes were freshly loaded with the viral mRNA. DDX3 was not found in the 80S fractions when we applied a translation-defective mutant HCV mRNA to the assay (Supplementary Figure S5).

While these data suggested that DDX3 associated specifically with newly-formed, i.e. mRNA-containing 80S

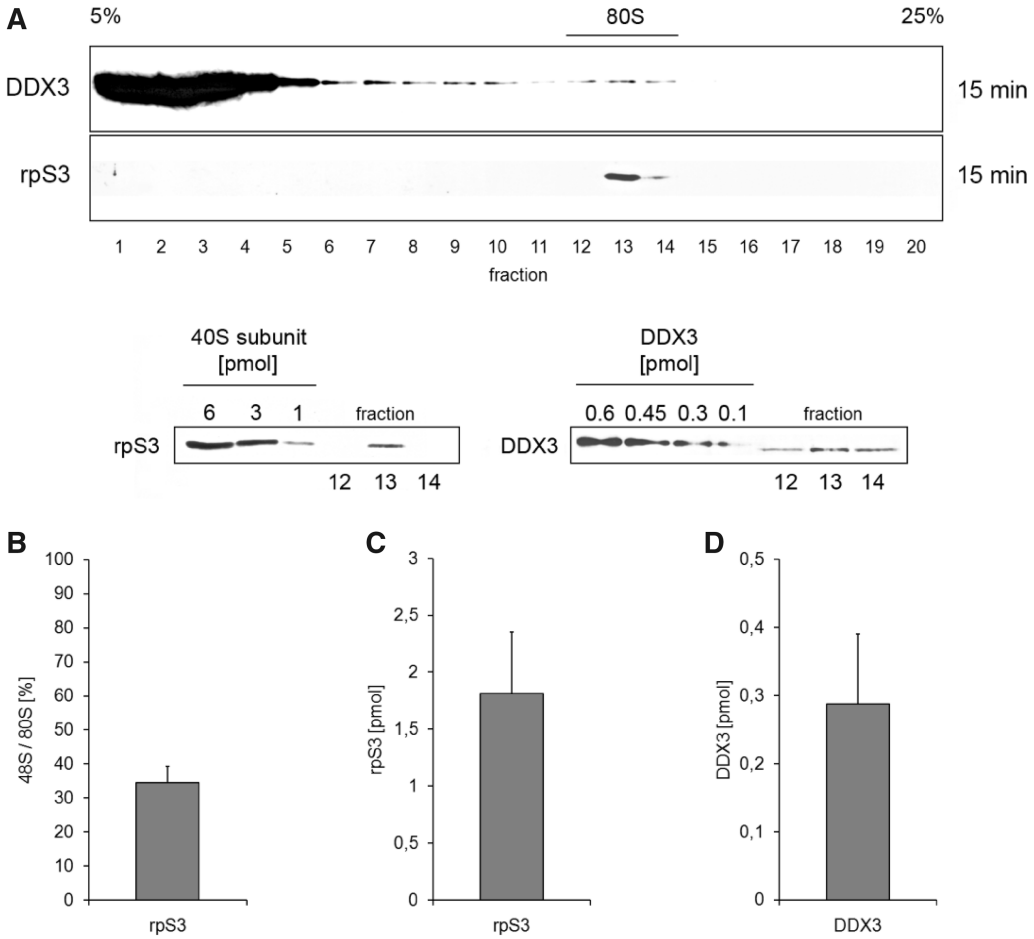

Figure 6. Estimating the amount of DDX3 that associates with newly assembled 80S ribosomes. (**A**) (Upper panel) Representative immunoblot of gradient fractions of a translation initiation reaction on capped mRNA at 15 min that was used to estimate the amounts of rpS3 and DDX3 in the 80S fractions. At this time all rpS3 sediments at 80S. (Lower panel) The molar amounts of rpS3 and of DDX3 in 48S and 80S fractions were established by comparing the western blot signals in the corresponding gradient fractions with signals obtained with known quantities of purified 40S subunits and recombinant DDX3, respectively. The recombinant DDX3 contains an additional tag and hence is slightly bigger than the natural DDX3. (**B**, **C** and **D**) Data from gradients of three independent translation initiation experiments were used to estimate the percentile (B) of newly assembled 80S translation initiation complexes, (C) the calculated molar amount of 80S ribosomal complexes at 15 min translation initiation, and (D) the calculated molar amount of DDX3 in newly assembled 80S complexes. (B) Translation initiation reactions were carried out for 20 s and the amounts of rpS3 (representing the 40S subunits) determined in the 48S and 80S peak fractions (fractions 7, 8 and 12), respectively (see Figure 5B for a representative gradient). The bar graph represents the percentage of 40S subunits in 48S complexes (i.e. the proportion that is capable of assembly into new 80S complexes) in relation to the sum of 40S subunits detectable in the 48S and 80S fractions. (C) Bar graph showing the molar amount of 40S subunits that was assessed to be present in the 80S fractions at 15 min translation initiation (i.e. total number of 80S complexes in fractions 12–14 of Figure 6A). (D) Bar graph representing the molar amount of DDX3 that was found to be associated with newly assembled 80S translation initiation complexes at 15 min translation initiation. Considering that ~35% (according to Figure 6B), i.e. ~0.6 pmol (according to Figure 6C) of the 80S complexes corresponded to newly assembled 80S translation initiation complexes, DDX3 interacted with 0.3 pmol (~50%) of these complexes (giving a 1:1 molar ratio of ribosomes:DDX3). Error bars indicate standard deviation of three independent experiments.

translation initiation complexes, we next sought to gain an idea on the quantity of DDX3 involved in this process. This was considered important, as only a small fraction of the total amount of cytoplasmic DDX3 cofractionated with the translation machinery (Figures 3 and 5B). For this, it was first essential to determine the percentage of ribosomes that were newly assembled on mRNA molecules during the course of the performed translation initiation reaction. We therefore repeated the assay shown in Figure 5B and measured at 20 s the amounts of rpS3 (reflecting the number of 40S subunits) in the 48S initiation complexes in relation to the sum of rpS3 that were immuno-detectable in the 48S and 80S complexes at this time point. It became apparent that only ~35% of the total of 40S subunits were present in 48S complexes and destined to form 80S translation initiation complexes (Figure 6B; see Figure 5B for a representative gradient profile). This number was in general agreement with earlier reports that estimated the number of 'free' (i.e. residual, non-active) 80S ribosomes to ~70% of the cytoplasmic ribosomes (28–30). Assessing now the total number of 80S ribosomes at 15 min translation initiation (Figure 6C) and the number of DDX3 molecules that cofractioned in the 80S fractions at this time, we could estimate that ~50% of the newly assembled ribosomes contained DDX3 (Figure 6D). This calculation revealed

that the small fraction of cytoplasmic DDX3 that associates with the translation machinery nevertheless is sufficient to saturate a significant number of functional ribosomes.

Finally, we addressed the question whether the observed translocation of DDX3 into mRNA-containing 80S ribosomes was possibly caused by a non-specific association of the protein to the mRNA. For this purpose, we treated newly assembled translation initiation complexes with MN and analyzed these in the above-described manner (see Supplementary Figure S6). The MN was confirmed to be fully active under the conditions of the translation initiation reaction, and the integrity of the 80S complexes remained, as expected, nearly unaffected by the nuclease-treatment. Interestingly, DDX3 remained detectable at 80S also after MN-treatment, which suggested a direct, non-RNA-mediated interaction of the protein with newly assembled 80S ribosomes (Supplementary Figure S6).

Taken together, these observations implied an evident function of DDX3 in translation initiation. That is, the protein was indicated to be entailed in either the formation of the 48S or of the 80S initiation complexes (Figure 1 steps ① or ②). The fact that DDX3 was not associated with 'free' monomeric 80S ribosomes that were detectable at all time points of the initiation reaction (Figure 5B, fraction 12; Supplementary Figure S5, fractions 13 and 14) further suggested that the protein does not participate in ribosome recycling.

DDX3 promotes the assembly of functional 80S ribosomes

The following experiments were aimed at dissecting if DDX3 is involved in 48S or 80S complex formation of the translation initiation process. For this purpose, we prepared cytoplasmic S10 extracts from Huh7 cells where the level of DDX3 had been significantly reduced to ~25% of the original level by prior treatment of the cells with one of the DDX3-specific siRNAs (Figure 7A). In accordance with the earlier cell transfection studies (Figure 2), *in vitro* translation experiments with such 'DDX3-depleted' extracts and reporter mRNAs showed a translation activity that was ~35–50% lower than that of mock-depleted extracts (Supplementary Figure S7).

In the first test of this series we compared translation initiation in the DDX3- and mock-depleted extract using the same assays as above (Figure 5 and Supplementary Figure S5) and capped- and HCV IRES-containing mRNAs as substrates. Again, these experiments resulted in analogous data with both mRNAs: i.e. the DDX3 knock down had no effect on the formation of the 48S complexes at the early time point (Figure 7B and D). However, at longer reaction times and compared to the non-depleted control extracts, the amounts of newly assembled 80S ribosomes were reduced by ~40% in the DDX3-depleted extracts (Figure 7C and E). Conversely, the total of 48S complexes was increased in the DDX3-depleted extracts, i.e. by an average factor of 1.3 (capped RNA) and 1.54 (HCV IRES-RNA), respectively. These results supported the concept that DDX3 accelerates the assembly of functional 80S ribosomal complexes during translation initiation. This conclusion was further confirmed by toe printing experiments, which showed that the depletion of DDX3 did not affect the formation of the 48S complex (Supplementary Figure S8).

The final experiment was directed to examine the effect of DDX3 on the assembly of 48S and 80S translation initiation complexes *in vitro*. For this purpose, we applied the above-described affinity-purified Flag-DDX3 and the corresponding mock-purified control (Figure 4C and Supplementary Figure S9D). As mentioned above, the purified Flag-DDX3 was confirmed to be free of translation initiation factors and ribosomal subunits; immunoblots excluded contaminations with eIF2, eIF3, eIF5, 40S and 60S, and a translation initiation experiment performed with the DDX3-containing protein fraction revealed no residual formation of 48S and 80S complexes, respectively (Supplementary Figure S9F). To investigate if the purified Flag-DDX3 affected the 48S assembly process, purified eIF3 and 40S subunits were coincubated with Met–$tRNA_i^{Met}$ under translation initiation conditions with labeled HCV 5′-UTR-sORF-3′-UTR RNA and *in vitro* formed 48S complexes monitored by gradient centrifugation. As expected from our earlier data, formation of 48S complexes occurred, irrespective of whether the experiment was supplemented with Flag-DDX3 or with the corresponding fractions of a mock-purification (Figure 7F, fractions 8 and 9). However, when we further supplemented the mixture with purified $eIF5B_{587–1220}$ and 60S subunits using the protocol of Terenin *et al.* (31) that enables the reconstitution of 80S ribosomes in the absence of eIF2, the 80S assembly occurred at considerably higher efficiency when Flag-DDX3 was present in the reaction (Figure 7G).

In sum, we concluded from these results that DDX3 functions as an auxiliary translation factor that promotes the assembly of functional 80S ribosomes (Figure 1 step ②).

DISCUSSION

The DEAD-box helicase DDX3 is involved in most steps of cellular gene expression. It was indicated to participate in the regulation of transcription of defined promoters (32–34), to shuttle between nucleus and cytoplasm and to accelerate the nuclear export of specific RNAs (7,35). Data obtained with one of several DDX3 yeast homologs, Ded1, revealed that this protein is necessary for translation initiation (36), and there is evidence that Ded1 operates in an mRNA specific manner, during 5′-UTR-unwinding and/or during mRNP remodeling (37–39). DDX3 was suggested to function in a similar way as Ded1 since it was also found to be important for translation and to interact with translation initiation factors (see Introduction section and Figure 4). However, its precise function remained elusive.

Taking advantage of moderate DDX3 knock down procedures (see below) we initiated this study by investigating the impact of the protein on the translation and replication of HCV RNA in Huh7 cells. Comparing transiently and persistently transfected HCV RNAs, we observed in

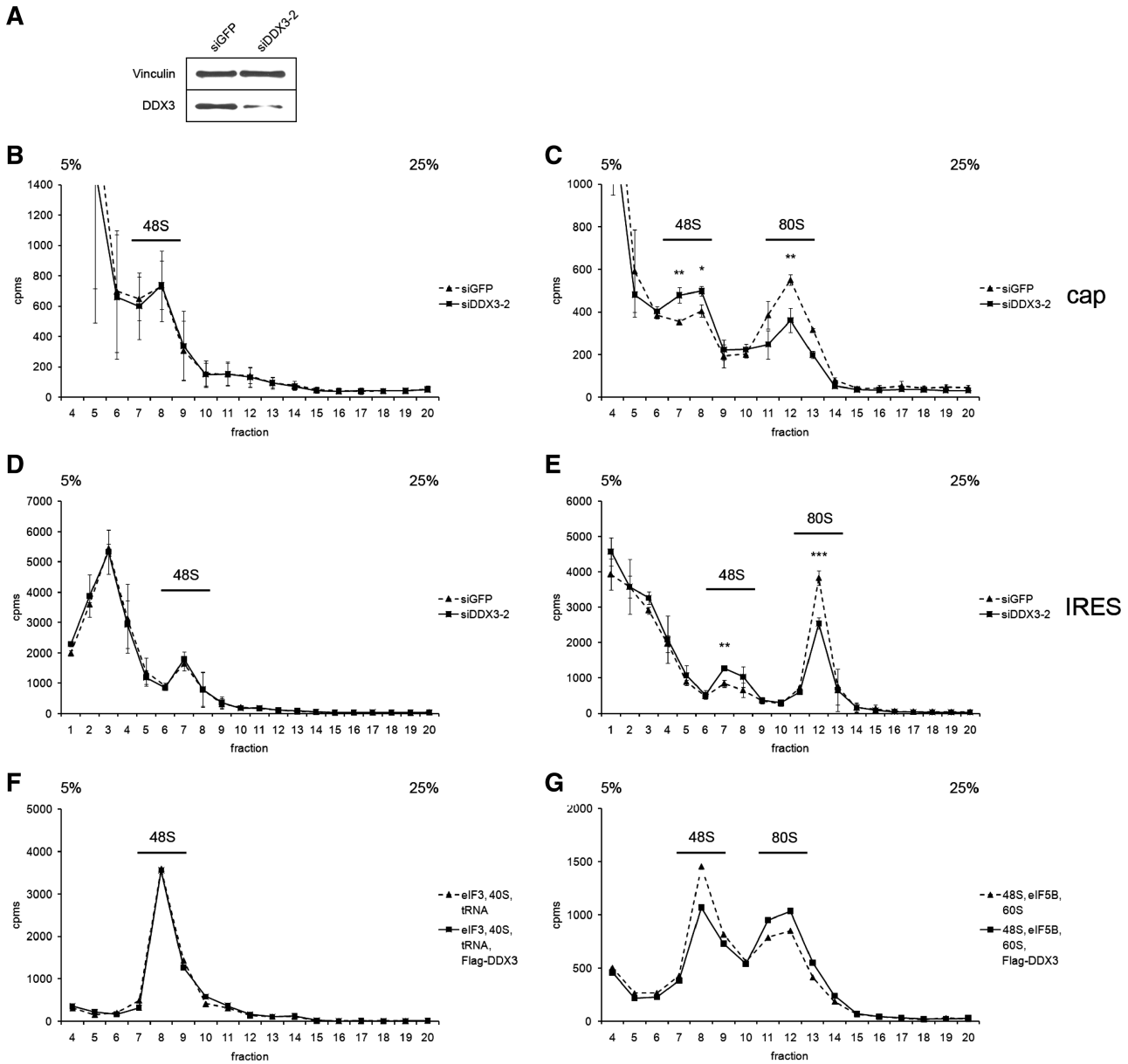

Figure 7. DDX3 promotes the assembly of functional 80S ribosomes. (**A**) Western blot analyses indicating the amounts of vinculin and of DDX3 in S10 extracts of Huh7 cells that were pre-treated with siGFP or siDDX3-2. (B–E) Translation initiation assays performed with mock-depleted and DDX3-depleted S10 extracts; formation of the 48S and 80S translation initiation complexes was monitored on [^{32}P]-labeled substrate RNA (Figure 5). (**B**) 48S and (**C**) 80S complex assembly on 5′cap-sORF-poly A at 20 s and 10 min, respectively (top gradient fractions omitted for better resolution). (**D**) 48S and (**E**) 80S complex assembly on HCV 5′-UTR-sORF-3′-UTR RNA at 1 and 10 min, respectively. Dashed line/triangles: data obtained with mock-depleted extract. Continuous line/squares: data obtained with DDX3-depleted extract. Error bars represent standard deviation of six independent experiments, (*) $P \leq 0.05$, (**) $P \leq 0.01$, (***) $P \leq 0.001$. Differences in the amounts of formed 48S and 80S translation initiation complexes were estimated by comparing the measured radioactivity in the 48S and 80S peak fractions. (**F** and **G**) *In vitro* assembly of translation initiation complexes on [^{32}P]-labeled HCV RNA. Following the protocol of Terenin *et al.* (31) (see also Supplementary Figure S9), 48S complexes were assembled on the template using purified eIF3, Met–tRNA$_i^{Met}$ and 40S subunits in the presence and absence of purified Flag-DDX3, respectively (F). For the assembly of 80S complexes (G), the 48S complexes were further incubated with purified eIF5B$_{587–1220}$ and 60S ribosomal subunits, respectively. The assembled 48S and 80S complexes were separated by centrifugation through a 5–25% linear sucrose density gradient and the positions are indicated. One representative experiment is shown.

each case a significant reduction of protein synthesis in the DDX3-depleted cells, which revealed an evident role of DDX3 in HCV IRES- as well as EMCV IRES-directed translation (Figure 2). The fact that a reduction of cytoplasmic DDX3 inhibited the replication of transiently transfected HCV RNAs but not of persistently transfected replicons was attributed to different concentrations of viral replicase in the cells.

It is important to note that the DDX3 knock down experiments were performed with two different siRNAs that reduced the intracellular amount of DDX3 to ~15–25% of the original level (Figures 2 and 7).

We stayed with this depletion protocol since more effective siRNAs inhibited cell growth (unpublished observations). However, the remaining endogenous DDX3 certainly compromised the level of the measured effects. Despite this technical downside, we obtained further, comprehensive evidence supporting the notion that DDX3 functions to generally promote translation. That is, negative effects of DDX3 depletion on protein synthesis were measured irrespective of whether translation was monitored *in vivo* or *in vitro*, whether we applied different cap- or IRES-containing, short or long RNAs, and irrespective of whether the 5′-UTRs of the RNAs were structured or not (Figures 2 and 7, Supplementary Figures S2 and S7; e.g. the 5′-UTR of the most frequently used 5′cap-sORF-poly A mRNA is not structured). Hence, our findings are in accord with those reports that indicated a positive role of DDX3 in translation. They were in contrast to data of Shih *et al*. (5) who observed a translational repression with overexpressed DDX3. This discrepancy may be explained by adverse effects of large quantities of helicase proteins in the cell. Alternatively, it is conceivable that DDX3 overexpression blocks translation by the assembly of mRNA complexes that accumulate in stress granules, as it was recently shown with Ded1 (39). Actually, we found that a moderate overexpression of DDX3 stimulated translation (see Supplementary Figure S4). Our data also deviate in certain aspects from the report of Lai *et al*. (7). Using DDX3 knock down cells, these authors observed discrepancies in the translation of reporter mRNAs with differently structured 5′-UTRs and hypothesized a role of DDX3 in the scanning process. In our study, despite all types of mRNAs (with structured as well as with non-structured 5′-UTRs) were present in the DDX3-containing translation initiation complexes (Figure 4B), the fact that a depletion of the protein also inhibited IRES-mediated translation initiation, which does not involve scanning, strongly argues against a role of DDX3 in scanning (Figure 2G and Supplementary Figure S2A). DDX3 thus operates differently from the DEAH-box helicase DHX29, which was demonstrated to increase the processivity of scanning (40). Since DDX3 knock down inhibited translation regardless of whether the RNA substrates contained a 3′-UTR or a poly A tail, this also excluded DDX3 to be a functional part of RNA 5′–3′ interactions (Figure 2). Further experiments indicated that DDX3 neither is a component of translating polysomes (Figure 3) nor of 'free' 80S ribosomes (Figures 5 and 6). Together, these observations suggest that DDX3 does not contribute to the translation elongation or ribosome recycling processes.

Instead, our study supports the notion that DDX3 functions in the second step of translation initiation, the formation of the 80S translation initiation complex. Initial indications pointing in this direction came from the observation that DDX3 is not part of 'free' ribosomes, and that a fraction of the protein specifically joins newly assembled (i.e. mRNA-containing) 80S ribosomes (Figure 5 and Supplementary Figure S5). Convincing evidence for such a role of DDX3 was obtained with S10 extracts of DDX3 depleted cells where the assembly of functional 80S ribosomes was disabled (Figure 7C and E). In further support of this, 80S assembly from individual translation initiation compounds was enhanced in the presence of the purified protein (Figure 7G). Conversely, formation of 48S translation initiation complexes was unaffected by DDX3 (Figure 7B, D and F; Supplementary Figure S8). However, different experimental setups demonstrated that DDX3 specifically binds to eIF3 and to the 40S subunit, which fuels the assumption that DDX3 is a component of 43S PIC and, as such, becomes also part of 48S translation initiation complexes (Figures 3–5).

The portion of DDX3 that cosedimented with the translation machinery was small with respect to the total cytoplasmic amount of the protein (Figures 3–5). This was not surprising considering the high abundance of the protein in the cell and its multifunctional character. However, our semi-quantitative estimations indicated that at least 50% of the newly assembled 80S ribosomes contained DDX3 (Figure 6). It hence appears that this amount of DDX3 suffices to saturate a significant number of 40S/48S and newly formed 80S complexes, respectively, and to support efficient 80S assembly. In fact, the helicase protein DHX29, which is also involved in translation, was found to be associated with only 10% of the total number of 40S subunits (40).

Currently, one can only speculate about the molecular activity of DDX3 in 80S assembly. As the protein binds directly, i.e. in an RNA-independent manner to eIF3, to the 40S subunit and to the 80S initiation complex (Figure 4 and Supplementary Figure S6), respectively, it may act as a protein-bridge between different factors required for 40S/60S interactions. This concept is in accord with the current opinion of main functions of DEAD-box helicases (41–43), and it strikingly resembles a scenario that was proposed for the Drosophila DEAD box protein Vasa. Vasa was indicated to assist the recruitment of eIF5B to the 40S subunit and thus to facilitate translation of certain mRNAs (44). The idea that DDX3 acts as a protein-bridge moreover fits with observations in overexpression assays where not only the wild-type DDX3 was found to induce translation (see above) but also a variant with defective helicase and ATPase domains (Supplementary Figure S4). This suggests that the helicase and ATPase activities of DDX3 are not essential for its function in translation.

A particularly interesting aspect concerns the direct and stable interaction of DDX3 with eIF3. In translation initiation experiments with the HCV IRES, Pestova *et al*. (3) showed that eIF3 was not essential for 48S complex assembly but required for 80S complex formation. eIF3 was accordingly speculated to modify the conformation of the 48S complex such that a 60S subunit can associate (3,31). Thus, a potential model of DDX3 function is that the protein, by interacting with eIF3 and the 40S subunit and as part of the 43S PIC enters the 48S complex on translatable mRNA. Then, in conjunction with eIF3, DDX3 may operate as a conformational modulator of the 48S complex supporting 80S assembly by protein–protein interactions. While eIF3 leaves the 48S complex during assembly of the 80S translation initiation complex, DDX3 remains bound to it but disassembles prior to the elongation process (Figure 1).

With DDX3, this study implicates another helicase, which, besides eIF4A and DHX29, has a defined role in mammalian cellular protein synthesis.

SUPPLEMENTARY DATA

Supplementary Data are available at NAR Online: Supplementary Materials and Methods, Supplementary Figures 1–9, Supplementary Tables 1–2 and Supplementary References (9,13,46–51).

ACKNOWLEDGEMENTS

The authors thank Christine Hamann for technical support, Reinhard Lührmannn for HeLa extracts and Elmar Wahle for critical reading of the manuscript. We are grateful to Arvind H. Patel for significant intellectual impact in the paper and for anti-DDX3 antiserum.

FUNDING

National Institute of Health '(grant number 5-RO1-DK-62847-3 to S.E.B)'; and the Deutsche Forschungsgemeinschaft '(grant number BE 1885/6 to R.G.). Funding for open access charge: Deutsche Forschungsgemeinschaft and Martin Luther University Halle-Wittenberg.

Conflict of interest statement. None declared.

REFERENCES

1. Sonenberg,N. and Hinnebusch,A.G. (2009) Regulation of translation initiation in eukaryotes: mechanisms and biological targets. *Cell*, **136**, 731–745.
2. Jackson,R.J., Hellen,C.U. and Pestova,T.V. (2010) The mechanism of eukaryotic translation initiation and principles of its regulation. *Nat. Rev. Mol. Cell Biol.*, **11**, 113–127.
3. Pestova,T.V., Shatsky,I.N., Fletcher,S.P., Jackson,R.J. and Hellen,C.U. (1998) A prokaryotic-like mode of cytoplasmic eukaryotic ribosome binding to the initiation codon during internal translation initiation of hepatitis C and classical swine fever virus RNAs. *Genes Dev.*, **12**, 67–83.
4. Kieft,J.S., Zhou,K., Jubin,R. and Doudna,J.A. (2001) Mechanism of ribosome recruitment by hepatitis C IRES RNA. *RNA*, **7**, 194–206.
5. Shih,J.W., Tsai,T.Y., Chao,C.H. and Wu Lee,Y.H. (2008) Candidate tumor suppressor DDX3 RNA helicase specifically represses cap-dependent translation by acting as an eIF4E inhibitory protein. *Oncogene*, **27**, 700–714.
6. Lee,C.S., Dias,A.P., Jedrychowski,M., Patel,A.H., Hsu,J.L. and Reed,R. (2008) Human DDX3 functions in translation and interacts with the translation initiation factor eIF3. *Nucleic Acids Res.*, **36**, 4708–4718.
7. Lai,M.-C., Lee,Y.-H.W. and Tarn,W.-Y. (2008) The DEAD-box RNA helicase DDX3 associates with export messenger ribonucleoproteins as well as tip-associated protein and participates in translational control. *Mol. Biol. Cell.*, **19**, 3847–3858.
8. Tarn,W.Y. and Chang,T.H. (2009) The current understanding of Ded1p/DDX3 homologs from yeast to human. *RNA Biol.*, **6**, 17–20.
9. Grassmann,C.W., Yu,H., Isken,O. and Behrens,S.-E. (2005) Hepatitis C virus and the related bovine viral diarrhea virus considerably differ in the functional organization of the 5' non-translated region: implications for the viral life cycle. *Virology*, **333**, 349–366.
10. Geissler,R., Scholze,H., Hahn,S., Streubel,J., Bonas,U., Behrens,S.E. and Boch,J. (2011) Transcriptional activators of human genes with programmable DNA-specificity. *PLoS One*, **6**, e19509.
11. Yu,H., Isken,O., Grassmann,C.W. and Behrens,S.E. (2000) A stem-loop motif formed by the immediate 5' terminus of the bovine viral diarrhea virus genome modulates translation as well as replication of the viral RNA. *J. Virol.*, **74**, 5825–5835.
12. Isken,O., Baroth,M., Grassmann,C.W., Weinlich,S., Ostareck,D.H., Ostareck-Lederer,A. and Behrens,S.E. (2007) Nuclear factors are involved in hepatitis C virus RNA replication. *RNA*, **13**, 1675–1692.
13. Pisarev,A.V., Unbehaun,A., Hellen,C.U. and Pestova,T.V. (2007) Assembly and analysis of eukaryotic translation initiation complexes. *Meth. Enzymol.*, **430**, 147–177.
14. Damoc,E., Fraser,C.S., Zhou,M., Videler,H., Mayeur,G.L., Hershey,J.W., Doudna,J.A., Robinson,C.V. and Leary,J.A. (2007) Structural characterization of the human eukaryotic initiation factor 3 protein complex by mass spectrometry. *Mol. Cell. Proteomics*, **6**, 1135–1146.
15. Stoyan,T., Michaelis,U., Schooltink,H., Van Dam,M., Rudolph,R., Heinrich,P.C. and Rose-John,S. (1993) Recombinant soluble human interleukin-6 receptor. Expression in Escherichia coli, renaturation and purification. *Eur. J. Biochem.*, **216**, 239–245.
16. Weidensdorfer,D., Stöhr,N., Baude,A., Lederer,M., Köhn,M., Schierhorn,A., Buchmeier,S., Wahle,E. and Huttelmaier,S. (2009) Control of c-myc mRNA stability by IGF2BP1-associated cytoplasmic RNPs. *RNA*, **15**, 104–115.
17. Angus,A.G., Dalrymple,D., Boulant,S., McGivern,D.R., Clayton,R.F., Scott,M.J., Adair,R., Graham,S., Owsianka,A.M., Targett-Adams,P. *et al.* (2010) Requirement of cellular DDX3 for hepatitis C virus replication is unrelated to its interaction with the viral core protein. *J. Gen. Virol.*, **91**, 122–132.
18. Harris,D., Zhang,Z., Chaubey,B. and Pandey,V.N. (2006) Identification of cellular factors associated with the 3′-nontranslated region of the hepatitis C virus genome. *Mol. Cell. Proteomics*, **5**, 1006–1018.
19. Ariumi,Y., Kuroki,M., Abe,K.-i., Dansako,H., Ikeda,M., Wakita,T. and Kato,N. (2007) DDX3 DEAD-box RNA helicase is required for hepatitis C virus RNA replication. *J. Virol.*, **81**, 13922–13926.
20. Randall,G., Panis,M., Cooper,J.D., Tellinghuisen,T.L., Sukhodolets,K.E., Pfeffer,S., Landthaler,M., Landgraf,P., Kan,S., Lindenbach,B.D. *et al.* (2007) Cellular cofactors affecting hepatitis C virus infection and replication. *Proc. Natl. Acad. Sci. USA*, **104**, 12884–12889.
21. Weinlich,S., Hüttelmaier,S., Schierhorn,A., Behrens,S.E., Ostareck-Lederer,A. and Ostareck,D.H. (2009) IGF2BP1 enhances HCV IRES-mediated translation initiation via the 3'UTR. *RNA*, **15**, 1528–1542.
22. Kato,T., Date,T., Miyamoto,M., Sugiyama,M., Tanaka,Y., Orito,E., Ohno,T., Sugihara,K., Hasegawa,I., Fujiwara,K. *et al.* (2005) Detection of anti-hepatitis C virus effects of interferon and ribavirin by a sensitive replicon system. *J. Clin. Microbiol.*, **43**, 5679–5684.
23. Quinkert,D., Bartenschlager,R. and Lohmann,V. (2005) Quantitative analysis of the hepatitis C virus replication complex. *J. Virol.*, **79**, 13594–13605.
24. Honda,M., Brown,E.A. and Lemon,S.M. (1996) Stability of a stem-loop involving the initiator AUG controls the efficiency of internal initiation of translation on hepatitis C virus RNA. *RNA*, **2**, 955–968.
25. Spahn,C.M., Kieft,J.S., Grassucci,R.A., Penczek,P.A., Zhou,K., Doudna,J.A. and Frank,J. (2001) Hepatitis C virus IRES RNA-induced changes in the conformation of the 40s ribosomal subunit. *Science*, **291**, 1959–1962.
26. Kaminski,A., Howell,M.T. and Jackson,R.J. (1990) Initiation of encephalomyocarditis virus RNA translation: the authentic initiation site is not selected by a scanning mechanism. *EMBO J.*, **9**, 3753–3759.
27. Ceci,M., Gaviraghi,C., Gorrini,C., Sala,L.A., Offenhauser,N., Marchisio,P.C. and Biffo,S. (2003) Release of eIF6 (p27BBP)

from the 60S subunit allows 80S ribosome assembly. *Nature*, **426**, 579–584.
28. Cooper,H.L., Berger,S.L. and Braverman,R. (1976) Free ribosomes in physiologically nondividing cells. Human peripheral lymphocytes. *J. Biol. Chem.*, **251**, 4891–4900.
29. Safer,B., Jagus,R. and Kemper,W.M. (1979) Analysis of initiation factor function in highly fractionated and unfractionated reticulocyte lysate systems. *Meth. Enzymol.*, **60**, 61–87.
30. Otto,G.A. and Puglisi,J.D. (2004) The pathway of HCV IRES-mediated translation initiation. *Cell*, **119**, 369–380.
31. Terenin,I.M., Dmitriev,S.E., Andreev,D.E. and Shatsky,I.N. (2008) Eukaryotic translation initiation machinery can operate in a bacterial-like mode without eIF2. *Nat. Struct. Mol. Biol.*, **15**, 836–841.
32. Schröder,M., Baran,M. and Bowie,A.G. (2008) Viral targeting of DEAD box protein 3 reveals its role in TBK1/IKKepsilon-mediated IRF activation. *EMBO J.*, **27**, 2147–2157.
33. Soulat,D., Bürckstümmer,T., Westermayer,S., Goncalves,A., Bauch,A., Stefanovic,A., Hantschel,O., Bennett,K.L., Decker,T. and Superti-Furga,G. (2008) The DEAD-box helicase DDX3X is a critical component of the TANK-binding kinase 1-dependent innate immune response. *EMBO J.*, **27**, 2135–2146.
34. Botlagunta,M., Vesuna,F., Mironchik,Y., Raman,A., Lisok,A., Winnard,P., Mukadam,S., Van Diest,P., Chen,J.H., Farabaugh,P. *et al.* (2008) Oncogenic role of DDX3 in breast cancer biogenesis. *Oncogene*, **27**, 3912–3922.
35. Yedavalli,V.S., Neuveut,C., Chi,Y.H., Kleiman,L. and Jeang,K.-T. (2004) Requirement of DDX3 DEAD box RNA helicase for HIV-1 Rev-RRE export function. *Cell*, **119**, 381–392.
36. Chuang,R.Y., Weaver,P.L., Liu,Z. and Chang,T.H. (1997) Requirement of the DEAD-Box protein ded1p for messenger RNA translation. *Science*, **275**, 1468–1471.
37. Noueiry,A.O., Chen,J. and Ahlquist,P. (2000) A mutant allele of essential, general translation initiation factor DED1 selectively inhibits translation of a viral mRNA. *Proc. Natl. Acad. Sci. USA*, **97**, 12985–12990.
38. Marsden,S., Nardelli,M., Linder,P. and McCarthy,J.E.G. (2006) Unwinding single RNA molecules using helicases involved in eukaryotic translation initiation. *J. Mol. Biol.*, **361**, 327–335.
39. Hilliker,A., Gao,Z., Jankowsky,E. and Parker,R. (2011) The DEAD-Box Protein Ded1 Modulates Translation by the Formation and Resolution of an eIF4F-mRNA Complex. *Mol. Cell*, **43**, 962–972.
40. Pisareva,V.P., Pisarev,A.V., Komar,A.A., Hellen,C.U.T. and Pestova,T.V. (2008) Translation initiation on mammalian mRNAs with structured 5'UTRs requires DExH-box protein DHX29. *Cell*, **135**, 1237–1250.
41. Gustafson,E.A. and Wessel,G.M. (2010) DEAD-box helicases: posttranslational regulation and function. *Biochem. Biophys. Res. Commun.*, **395**, 1–6.
42. Pyle,A.M. (2008) Translocation and unwinding mechanisms of RNA and DNA helicases. *Annu. Rev. Biophys.*, **37**, 317–336.
43. Schröder,M. (2010) Human DEAD-box protein 3 has multiple functions in gene regulation and cell cycle control and is a prime target for viral manipulation. *Biochem. Pharmacol.*, **79**, 297–306.
44. Liu,N., Han,H. and Lasko,P. (2009) Vasa promotes Drosophila germline stem cell differentiation by activating mei-P26 translation by directly interacting with a (U)-rich motif in its 3′ UTR. *Genes Dev.*, **23**, 2742–2752.
45. Lohmann,V., Körner,F., Koch,J., Herian,U., Theilmann,L. and Bartenschlager,R. (1999) Replication of subgenomic hepatitis C virus RNAs in a hepatoma cell line. *Science*, **285**, 110–113.
46. Iizuka,N., Najita,L., Franzusoff,A. and Sarnow,P. (1994) Cap-dependent and cap-independent translation by internal initiation of mRNAs in cell extracts prepared from Saccharomyces cerevisiae. *Mol. Cell. Biol.*, **14**, 7322–7330.
47. Naarmann,I.S., Harnisch,C., Flach,N., Kremmer,E., Kühn,H., Ostareck,D.H. and Ostareck-Lederer,A. (2008) mRNA silencing in human erythroid cell maturation: heterogeneous nuclear ribonucleoprotein K controls the expression of its regulator c-Src. *J. Biol. Chem.*, **283**, 18461–18472.
48. Shi,P.Y., Tilgner,M. and Lo,M.K. (2002) Construction and characterization of subgenomic replicons of New York strain of West Nile virus. *Virology*, **296**, 219–233.
49. Reich,S., Golbik,R.P., Geissler,R., Lilie,H. and Behrens,S.-E. (2010) Mechanisms of activity and inhibition of the hepatitis C virus RNA-dependent RNA polymerase. *J. Biol. Chem.*, **285**, 13685–13693.
50. Ostareck,D.H., Ostareck-Lederer,A., Shatsky,I.N. and Hentze,M.W. (2001) Lipoxygenase mRNA silencing in erythroid differentiation: The 3'UTR regulatory complex controls 60S ribosomal subunit joining. *Cell*, **104**, 281–290.
51. Cordin,O., Banroques,J., Tanner,N.K. and Linder,P. (2006) The DEAD-box protein family of RNA helicases. *Gene*, **367**, 17–37.